Neuron, Volume *99*

Supplemental Information

The Role of m^6A/m-RNA Methylation in Stress Response Regulation

Mareen Engel, Carola Eggert, Paul M. Kaplick, Matthias Eder, Simone Röh, Lisa Tietze, Christian Namendorf, Janine Arloth, Peter Weber, Monika Rex-Haffner, Shay Geula, Mira Jakovcevski, Jacob H. Hanna, Dena Leshkowitz, Manfred Uhr, Carsten T. Wotjak, Mathias V. Schmidt, Jan M. Deussing, Elisabeth B. Binder, and Alon Chen

Figure S1

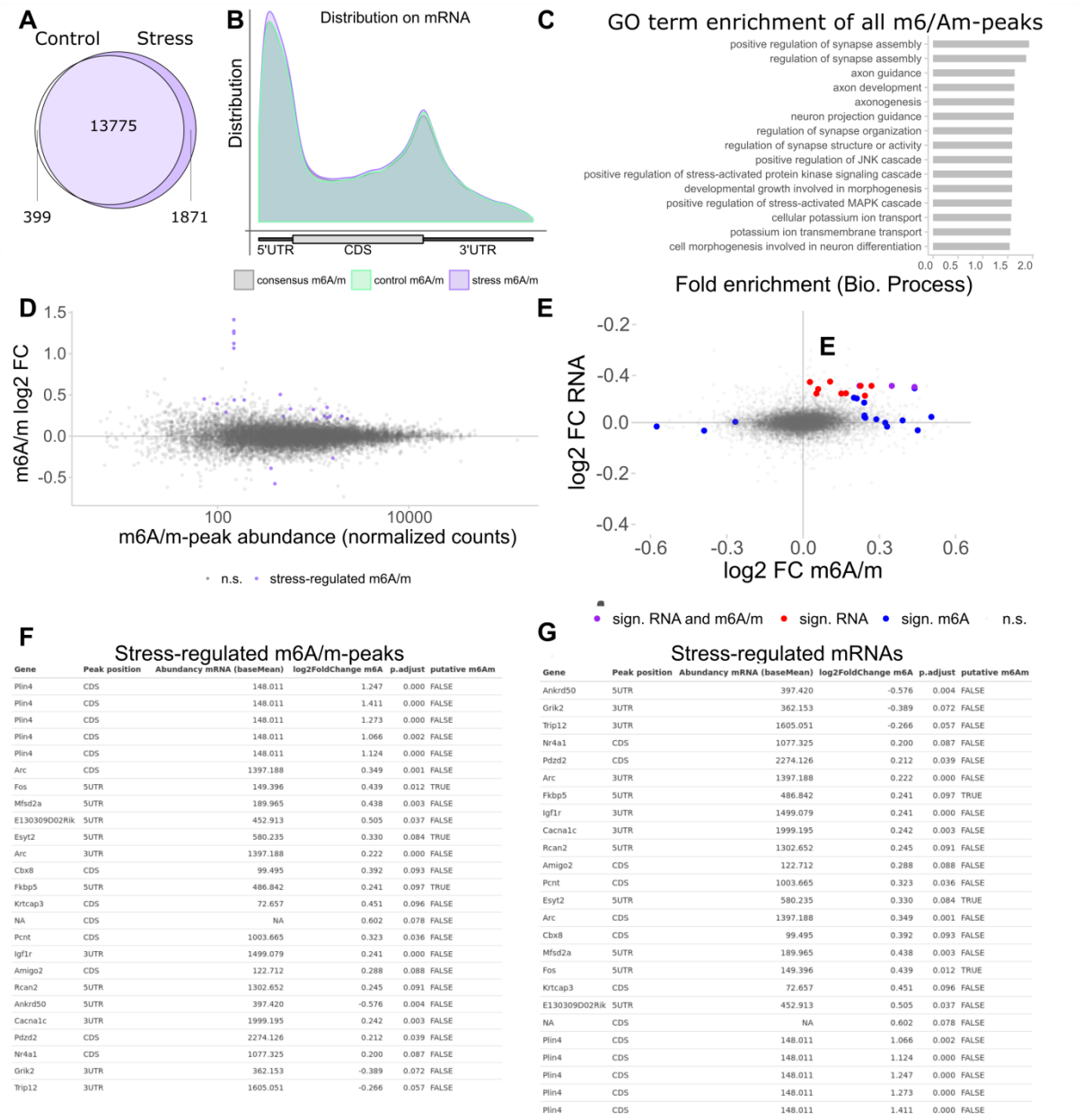

Gene	Peak position	Abundancy mRNA (baseMean)	log2FoldChange m6A	p.adjust	putative m6Am
Plin4	CDS	148.011	1.247	0.000	FALSE
Plin4	CDS	148.011	1.411	0.000	FALSE
Plin4	CDS	148.011	1.273	0.000	FALSE
Plin4	CDS	148.011	1.066	0.002	FALSE
Plin4	CDS	148.011	1.124	0.000	FALSE
Arc	CDS	1397.188	0.349	0.001	FALSE
Fos	5UTR	149.396	0.439	0.012	TRUE
Mfsd2a	5UTR	189.965	0.438	0.003	FALSE
E130309D02Rik	5UTR	452.913	0.505	0.037	FALSE
Esyt2	5UTR	580.235	0.330	0.084	TRUE
Arc	3UTR	1397.188	0.222	0.000	FALSE
Cbx8	CDS	99.495	0.392	0.093	FALSE
Fkbp5	5UTR	486.842	0.241	0.097	TRUE
Krtcap3	CDS	72.657	0.451	0.096	FALSE
NA	CDS	NA	0.602	0.078	FALSE
Pcnt	CDS	1003.665	0.323	0.036	FALSE
Igf1r	3UTR	1499.079	0.241	0.000	FALSE
Amigo2	CDS	122.712	0.288	0.088	FALSE
Rcan2	5UTR	1302.652	0.245	0.091	FALSE
Ankrd50	5UTR	397.420	-0.576	0.004	FALSE
Cacna1c	3UTR	1999.195	0.242	0.003	FALSE
Pdzd2	CDS	2274.126	0.212	0.039	FALSE
Nr4a1	CDS	1077.325	0.200	0.087	FALSE
Grik2	3UTR	362.153	-0.389	0.072	FALSE
Trip12	3UTR	1605.051	-0.266	0.057	FALSE

Gene	Peak position	Abundancy mRNA (baseMean)	log2FoldChange m6A	p.adjust	putative m6Am
Ankrd50	5UTR	397.420	-0.576	0.004	FALSE
Grik2	3UTR	362.153	-0.389	0.072	FALSE
Trip12	3UTR	1605.051	-0.266	0.057	FALSE
Nr4a1	CDS	1077.325	0.200	0.087	FALSE
Pdzd2	CDS	2274.126	0.212	0.039	FALSE
Arc	3UTR	1397.188	0.222	0.000	FALSE
Fkbp5	5UTR	486.842	0.241	0.097	TRUE
Igf1r	3UTR	1499.079	0.241	0.000	FALSE
Cacna1c	3UTR	1999.195	0.242	0.003	FALSE
Rcan2	5UTR	1302.652	0.245	0.091	FALSE
Amigo2	CDS	122.712	0.288	0.088	FALSE
Pcnt	CDS	1003.665	0.323	0.036	FALSE
Esyt2	5UTR	580.235	0.330	0.084	TRUE
Arc	CDS	1397.188	0.349	0.001	FALSE
Cbx8	CDS	99.495	0.392	0.093	FALSE
Mfsd2a	5UTR	189.965	0.438	0.003	FALSE
Fos	5UTR	149.396	0.439	0.012	TRUE
Krtcap3	CDS	72.657	0.451	0.096	FALSE
E130309D02Rik	5UTR	452.913	0.505	0.037	FALSE
NA	CDS	NA	0.602	0.078	FALSE
Plin4	CDS	148.011	1.066	0.002	FALSE
Plin4	CDS	148.011	1.124	0.000	FALSE
Plin4	CDS	148.011	1.247	0.000	FALSE
Plin4	CDS	148.011	1.273	0.000	FALSE
Plin4	CDS	148.011	1.411	0.000	FALSE

Figure S1. Additional analysis of the m^{6}A/m-Seq data. Related to Figure 1.

FC= fold change

(A) m^{6}A/m-peaks detected in basal and stress cortex samples mostly overlap. Shown are number and overlap of detected peaks per condition (in minimum 2/3 of the samples without additional abundancy filters applied to consensus peaks.). Upon visual inspection condition-unique peaks consist of peaks close to calling-threshold rather than true condition-unique signatures.

(B) m^{6}A/m-peaks detected in basal and stress cortex samples have the same distribution on mRNA.

(C) m^{6}A/m- methylated genes are enriched for genes related to synaptic structures and to neuronal development. (15 highest enriched Biological Process gene ontology (GO)

terms. Overrepresentation test of m^6A/m-peaks compared to all genes detected in input samples with FDR-corrected Q < 0.1.)

(D) MA-Plot of stress-regulation of m^6A/m-peaks mapped by m^6A/m-peak abundance.

(E) Genes regulated by stress on m^6A/m level and RNA expression level only partially overlap (3) with no clear correlation between gene m^6A/m and RNA change. (GLM coefficient 0.04, $R^2 = 0.02$, P < 2*10^-16.)

(F) Full list of m^6A/m-peaks significantly regulated by acute stress.

(G) Full list of mRNAs significantly regulated by acute stress.

Figure S2

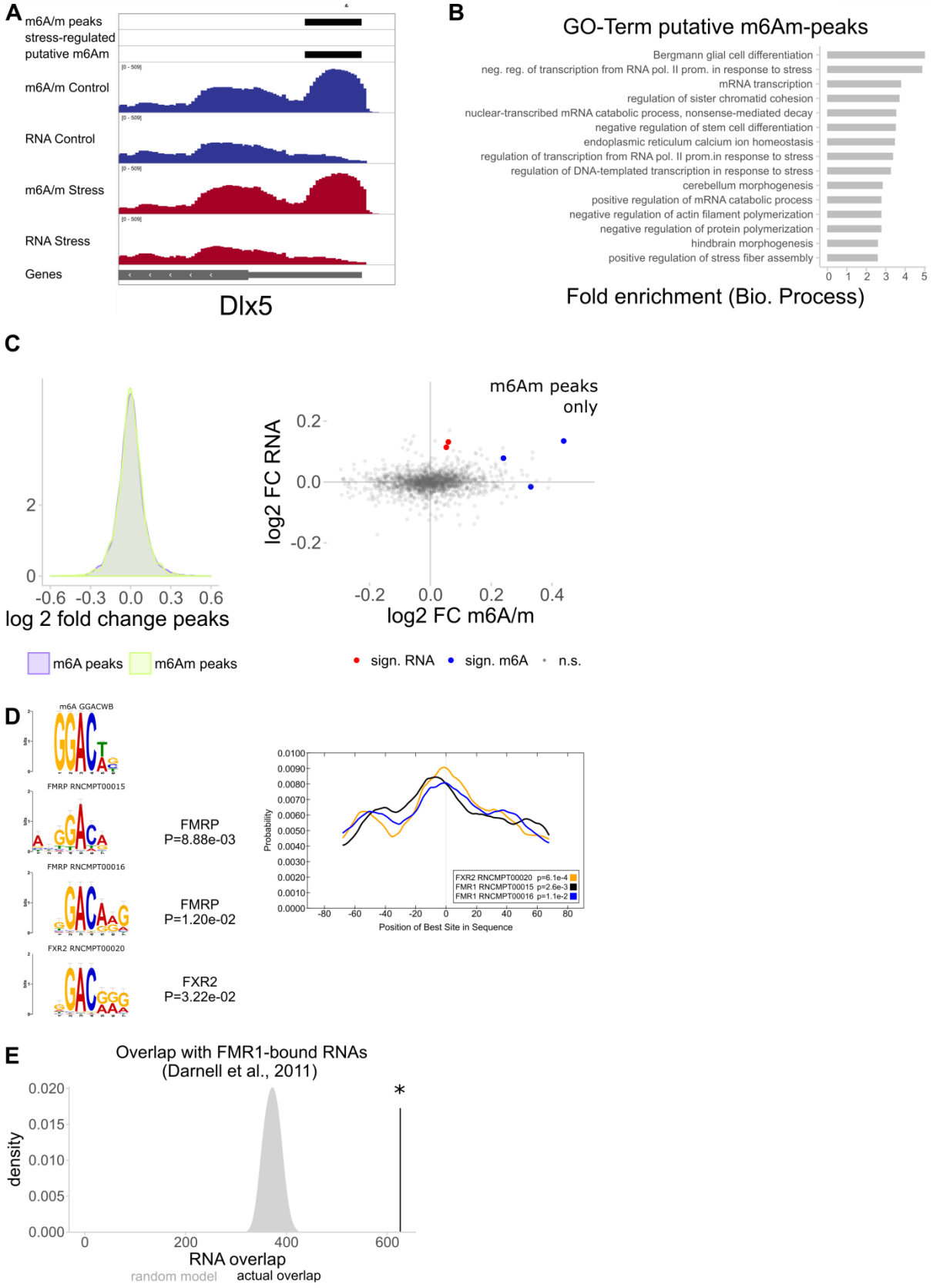

Figure S2. Additional analysis of the m^{6}A/m-Seq data, continued. Related to Figure 1.
FC= fold change

(A) Example of a putative m^6Am-peak shows the specific enrichment of m^6A-RIP reads at the transcription start site of m^6Am-peaks.
(B) In contrast to all m^6A/m-peaks, putative m^6Am peaks are more enriched for genes related to cellular stress response and RNA metabolism. (15 highest enriched Biological Process gene ontology (GO) terms. Overrepresentation test of putative m^6Am-peaks compared to all genes detected in input samples with FDR-corrected $Q < 0.1$.)
(C) Putative m^6Am peaks show similar fold changes as all m^6A/m-peaks and do also not correlate majorly with RNA change by stress. (GLM coefficient 0.03, $R^2 = 0.01$, $P <$ 1.12*10^-05).
(D) Comparing the m^6A-motif GGACWB to known motifs of RNA-binding proteins, 2 motifs for FMR1 as well as a motif for FXR2 are found to be most similar and centrally enriched in m^6A/m-peaks. FMR1 co-occurrence was not observed in putative m^6Am peaks. (Tomtom motif comparison results: FMR1 RNCMPT00015 (P = 8.88 *10^-03, E = 2.17), FMR1 RNCMPT00016 (P = 1.02 *10^-02, E = 2.93), FXR2 RNCMPT00020 (P = 3.22*10^-02, E = 8.37). All 3 motifs are centrally enriched in m^6A/m-peaks).
(E) Previously reported genes bound by mouse FMR1 are significantly enriched for m^6A/m-bound genes found in our study. (The amount of overlap observed (black line) was compared to distributions gained from 100 random permutations (grey distributions) of all observed expressed genes [Z-Test $P < 0.05$, analysis limited to genes detected in both data sets].)

Figure S3

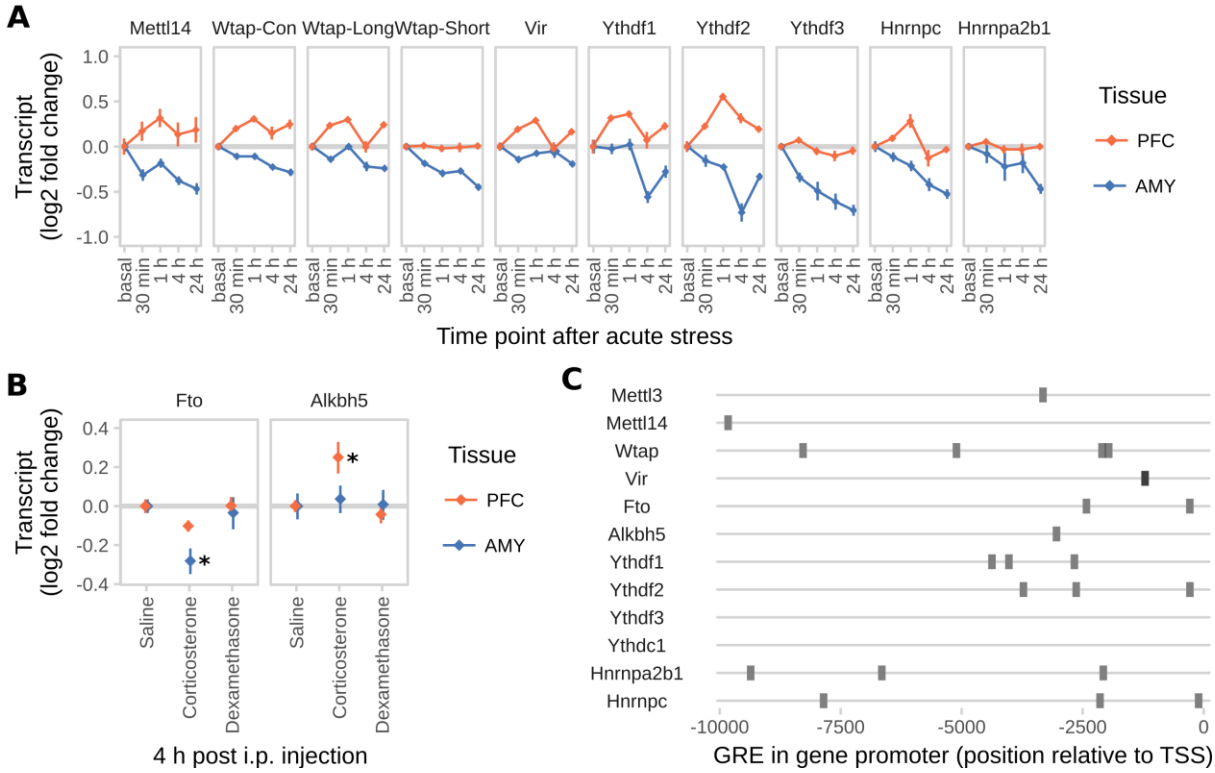

Figure S3. Acute injection of corticosterone i.p. leads to similar changes in global m^{6}A/m in the PFC and AMY like acute stress, suggesting that the effect on m^{6}A/m is mainly mediated by glucocorticoids. Related to Figure 2.

(A) Several m^{6}A/m-related genes are not regulated by acute stress indicating specificity of stress effects. Wtap expression is measured specifically for the long and short isoform as well as with primers measuring both (Con). (n = 12, log2 fold change ± SEM. 2-way MANOVA without significant interaction or main stress effects (FDR-corrected $P < 0.05$ and $n^2 > 0.01$). Full statistics see Supplementary Table 2.)

(B) Gene expression regulation of m^{6}A/m-demethylases Fto and Alkbh5 in the PFC and AMY shows similar patterns of regulation after corticosterone injection like after acute stress. (Fold change measured with qPCR; n = 12, mean ± SEM. Kruskal-Wallis-Test PFC Alkbh5 and AMY Fto $P < 0.05$, Stars: omnibus post-hoc comparisons to basal, $P < 0.065$).

(C) The majority of m^{6}A/m regulatory genes have upstream Glucocorticoid Response Elements (GRE). Prediction of high confidence GRE sites based on GRE consensus motif MA0113 10 kb upstream of the transcription start site (JASPAR, 90% relative profile score threshold).

Figure S4

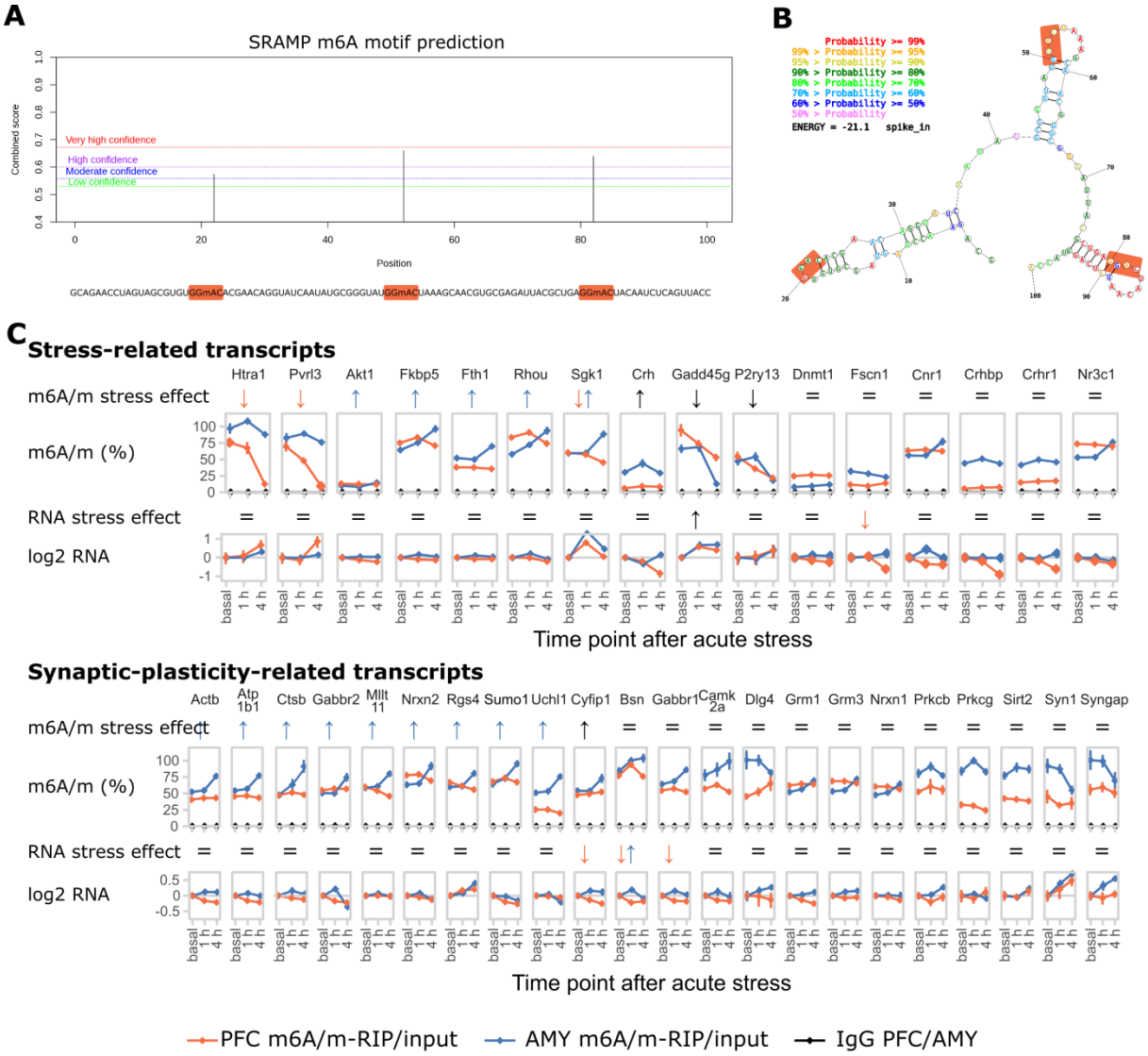

Figure S4. In-depth analysis of the m^{6}A/m-RIP-qPCR data. Related to Figure 3.

(A) Sequence and m^{6}A/m-site prediction of the synthetic spike-in oligo. The GGAC consensus motif containing the m^{6}A/m sites is marked up in the sequence string.

(B) Maximum free energy secondary structure of the oligo.

(C) Absolute full length m^{6}A/m-levels of stress-related and synaptic plasticity-related transcripts are differentially regulated in PFC and AMY of stress-related candidate transcripts and synaptic-plasticity-related candidate transcripts after stress. Extended data from Figure 3. % m^{6}A/m = % expression after precipitation relative to the total abundancy in input, normalized for immunoprecipitation efficiency by an internal methylated spike-in control. log2 RNA = log2 fold changes of transcript in input samples normalized to 5 housekeeping genes. (n = 8, mean ± SEM. Significant effects observed in FDR-corrected 2-way MANOVA ($P < 0.05$, $n^2 > 0.01$) are coded in the rows "m^{6}A/m stress effect" and "RNA stress effect": orange/blue arrows = PFC-/AMY-specific stress effect (interaction effect 2-way ANOVA, one-way follow up significant in respective tissue), black arrow = stress main stress

effect, equals sign = no interaction or stress main effect in 2-way ANOVA. For full statistics see Supplementary Table 2).

Figure S5

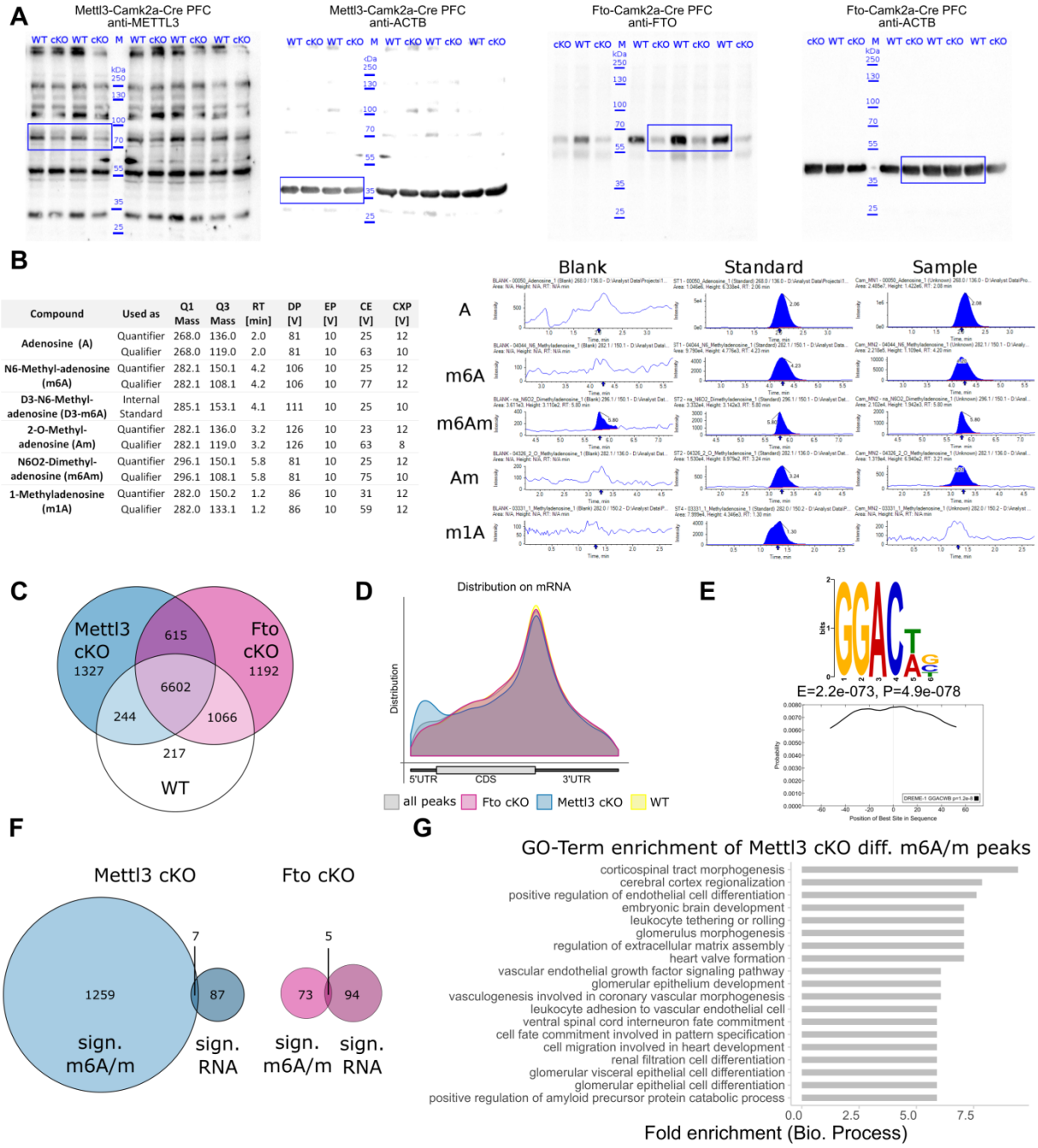

Compound	Used as	Q1 Mass	Q3 Mass	RT [min]	DP [V]	EP [V]	CE [V]	CXP [V]
Adenosine (A)	Quantifier	268.0	136.0	2.0	81	10	25	12
	Qualifier	268.0	119.0	2.0	81	10	63	10
N6-Methyl-adenosine (m6A)	Quantifier	282.1	150.1	4.2	106	10	25	12
	Qualifier	282.1	108.1	4.2	106	10	77	12
D3-N6-Methyl-adenosine (D3-m6A)	Internal Standard	285.1	153.1	4.1	111	10	25	10
2-O-Methyl-adenosine (Am)	Quantifier	282.1	136.0	3.2	126	10	23	12
	Qualifier	282.1	119.0	3.2	126	10	63	8
N6O2-Dimethyl-adenosine (m6Am)	Quantifier	296.1	150.1	5.8	81	10	25	12
	Qualifier	296.1	108.1	5.8	81	10	75	10
1-Methyladenosine (m1A)	Quantifier	282.0	150.2	1.2	86	10	31	12
	Qualifier	282.0	133.1	1.2	86	10	59	12

Figure S5. Additional analysis of Camk2a-Cre Mettl3 cKO and Camk2a-Cre Fto cKO mice. Related to Figure 4.

(A) Full blots of data shown in Figure 4B with bands spliced for the main figures and molecular weight marker shown in blue. Blots were first probed with anti-METTL3 or anti-FTO antibody and developed to show the full range of signal, and then stripped and re-probed with anti-ACTB antibody. Quantification shown in Figure 4B was performed on all samples using only the band at the marked up molecular weight (corresponding to the molecular weight of the protein).

(B) Measured nucleosides and parameters in LC-MS/MS including example traces for each one blank, synthetic standard and measured mouse mRNA per nucleoside. m^1A

could not be detected within quantitative measurement range in any of the measured mouse brain mRNAs.

(C) m^{6}A/m-peaks detected per group mostly overlap. Shown are number and overlap of detected peaks per group (in minimum 2/3 of the samples without additional abundancy filters applied to consensus peaks).

(D) m^{6}A/m-peaks detected per group as well as consensus peaks detected across all samples and used for differential methylation analysis have similar distribution on mRNA with a small enrichment of 5'UTR peaks specifically in Mettl3 cKO mRNA. (Peak distribution mapped along mRNA relative position).

(E) Consistent with the analysis of cortical m^{6}A/m after acute stress, GGACWB is the most abundant motif detected in m^{6}A/m-peaks and enriched at peak summits. Shown is the top detected sequence motif and its position across the detected m^{6}A/m-peaks.

(F) In addition to differentially methylated m^{6}A/m-peaks, several genes were detected differentially expressed in Mettl3 cKO and Fto cKO relative to WT animals, with low overlap between genes differentially methylated and differentially expressed and no clear correlation between m^{6}A/m methylation and gene expression (not shown).

(G) Genes differentially m^{6}A/m-methylated in Mettl3 cKO mRNA compared to WT are enriched for genes related to brain and tissue development. (15 highest enriched Biological Process gene ontology (GO) terms. Shown are Go terms overrepresented in m^{6}A/m-peaks genes compared to all genes detected in input samples with FDR-corrected Q < 0.1. Genes differentially m^{6}A/m-methylated in Fto cKO mRNA compared to WT did not result in any significantly enriched gene sets [not shown]).

Figure S6

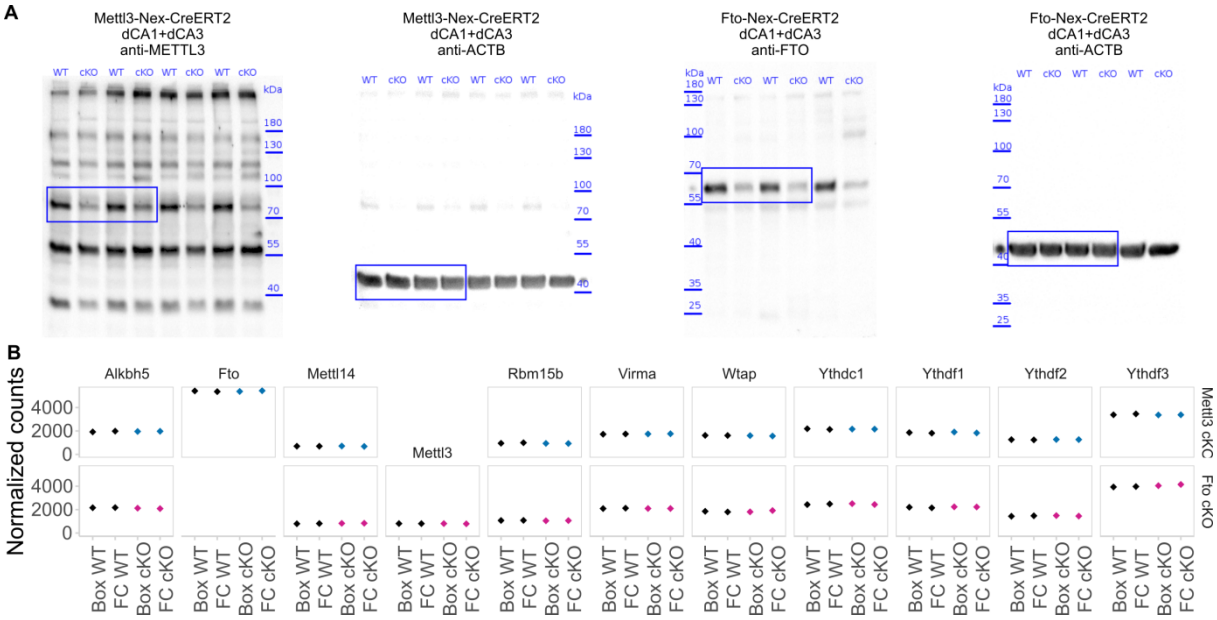

Figure S6. Additional analysis of Nex-CreERT2 Mettl3 cKO mice. Related to Figure 5.

(A) Full blots of data shown in Figure 5A with bands spliced for the main figures and molecular weight marker shown in blue. Blots were first probed with anti-METTL3 or anti-FTO antibody and developed to show the full range of signal, and then stripped and re-probed with anti-ACTB antibody. Quantification shown in Figure 5A was performed on all samples using only the band at the marked up molecular weight (corresponding to the molecular weight of the protein)

(B) Depletion of *Mettl3* or *Fto* in adult excitatory neurons is not compensated by changes of expression in other genes catalysing and or binding m^6A/m nor is the expression of those genes changed 24 hr after fear conditioning. (Normalized counts of genes plotted across both Mettl3 cKOs and Fto cKOs and respective wild type animals (WT) including animals 24 hr after fear conditioning (FC) and baseline animals (Box). n = 5. No significant genotype or fear-conditioning effects were detected at Q < 0.1).

Figure S7

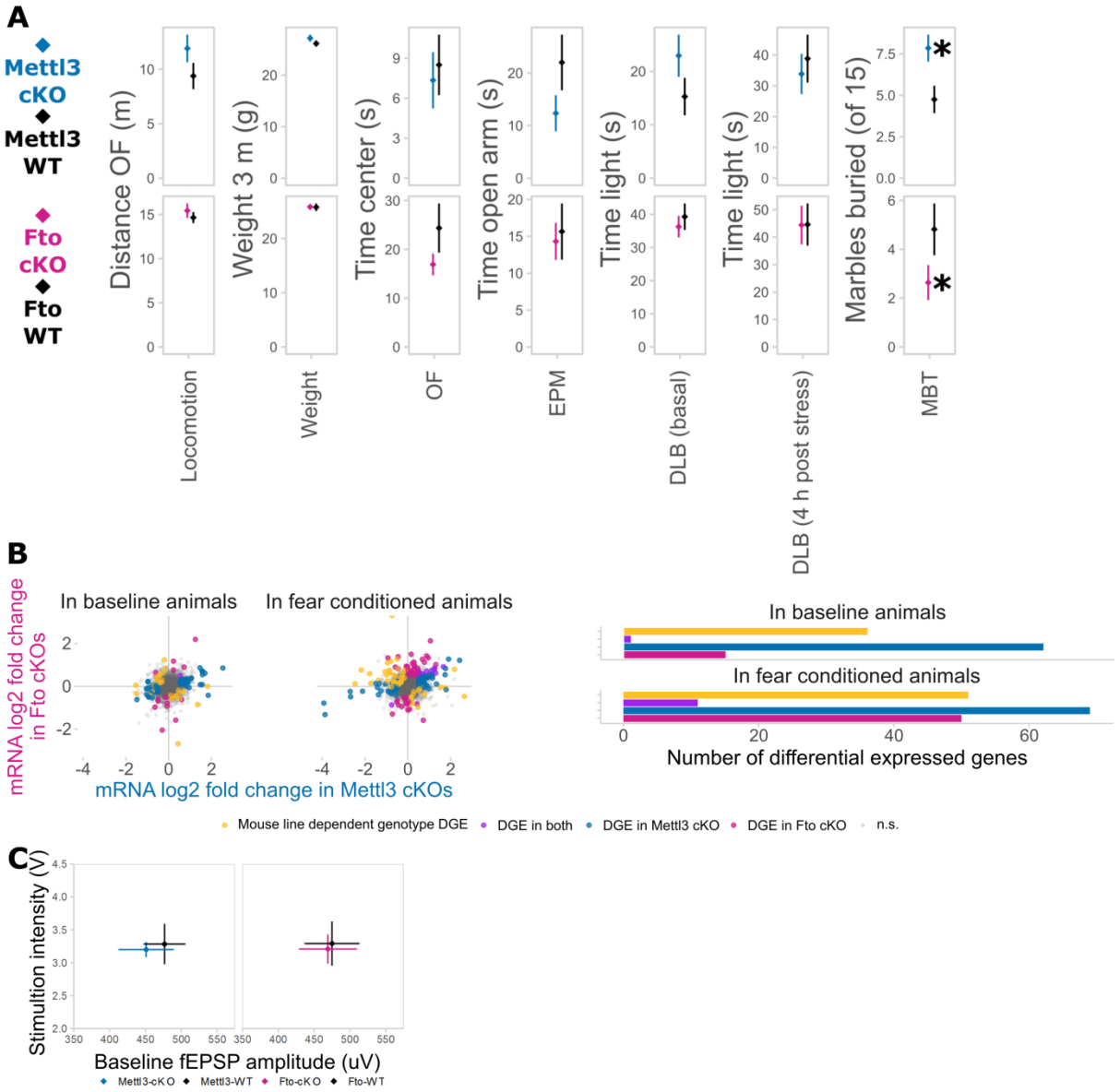

Figure S7. Anxiety-like behaviour is not changed in Mettl3 cKO and Fto cKO animals. Related to Figure 6.

(A) cKO animals did not differ in locomotion, weight or several measurements of anxiety-like behaviour, but spontaneous digging behaviour. OF = Open Field Test, EPM = Elevated Plus Maze, DLB = Dark Light Box, MBT = Marble Burying Test, WT = wild type animals, cKO = conditional knockout animals. Spontaneous burying behaviour as measured by the MBT was increased in Mettl3 cKO animals while decreased in Fto cKO animals. Weight 6 w post induction with Tamoxifen (average 12 w of age). Marbles buried within 10 min. (n = 11-13, mean ± SEM. * depict T-Tests P < 0.05).

(B) Gene expression changes in Mettl3 cKOs compared to their respective gene expression change in Fto cKOs are more diverse in fear conditioned animals than in baseline Box-control animals. The increase in differentially expressed genes after fear conditioning is larger in Fto cKO than in Mettl3 cKO mice. (Differentially expressed genes marked by colour: blue = genes differentially expressed in Mettl3 cKOs compared to WT,

pink = genes differentially expressed in Fto cKOs compared to WT, purple = genes differentially expressed in both, orange = genes expressed in a mouse line x genotype fashion. n = 5)

(C) Input/output properties of CA3-CA1 neurotransmission in Mettl3 cKO and Fto cKO are not altered. (Plotted are ranges baseline fEPSP in uV amplitudes to stimulation intensity in V, n = 10-12 slices from 5-6 animals, mean ± SEM).

Figure S8

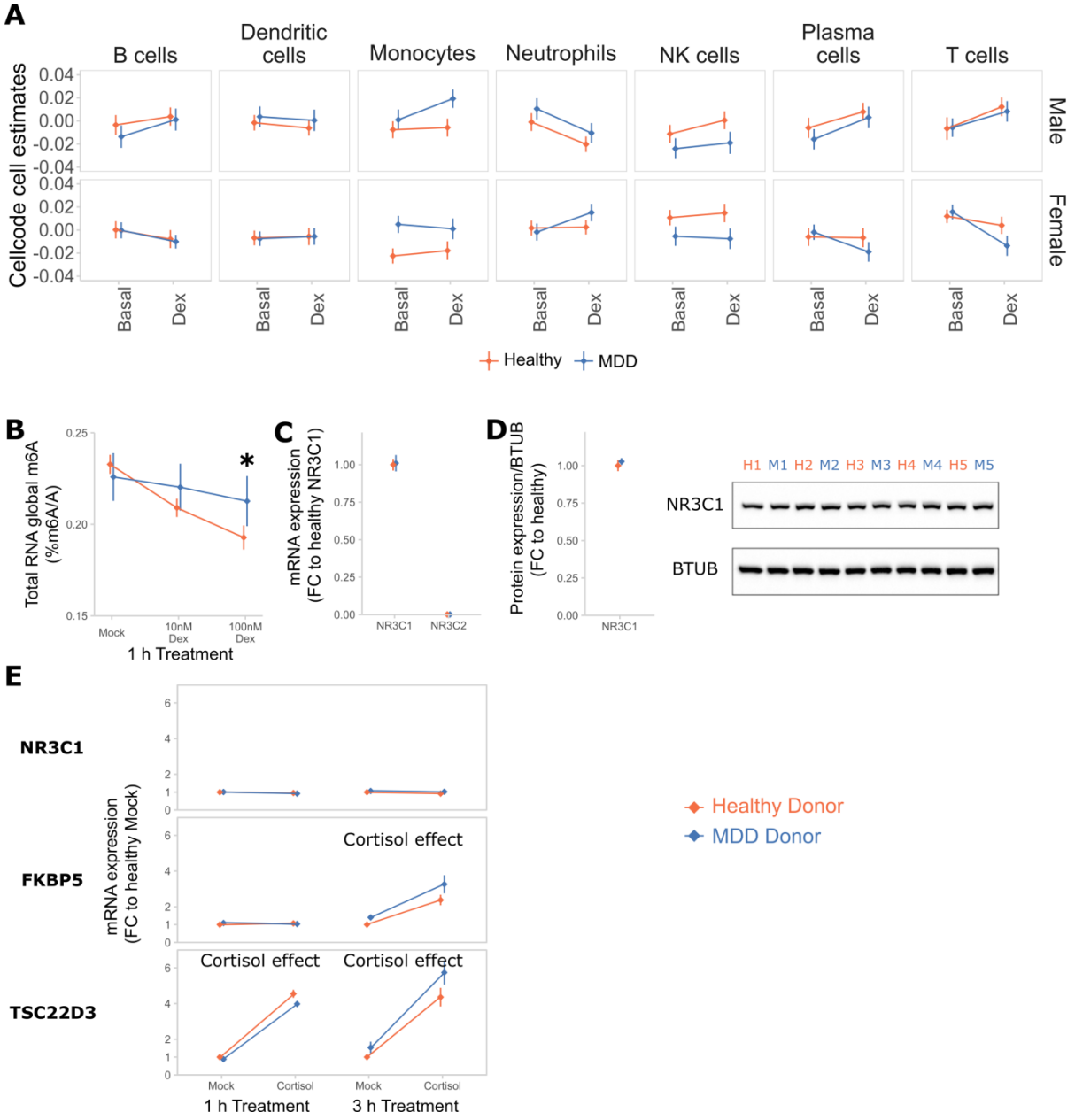

Figure S8. Additional data for Figures 6 and 7.

Dex = dexamethasone.

(A) Blood cell composition is not altered in blood samples used for m^{6}A/m **measurement.** (CellCODE cell composition estimates based on the residuals of the transcriptome-wide gene expression form the same blood samples used for Figure 7F did not yield any changes in blood cell composition by dexamethasone x diagnosis x sex interaction, dexamethasone x diagnosis interaction or dexamethasone main effects. Neutrophils, T cells, B cells and Plasma cells are significantly for sex x dexamethasone ($Q < 0.1$) which was however not regulated in the m^{6}A/m measurements. All blood samples used for m^{6}A/m measurements taken from Arloth et al., 2015.)

(B) Global m^{6}A/m in BLCLs after dexamethasone treatment is decreased in BLCLs from healthy, but not MDD-donors, similar of the effect of cortisol. (Global m^{6}A/m assay

on total RNA, n = 5 biological replicates with 3 technical replicates each, mean ± SEM. 2-way ANOVA: significant interaction effect of Dex and donor status ($F(3, 24) = 10.127$, $P = 0.001$). * depicts omnibus Tukey post-hoc tests to basal $P < 0.05$).

(C) BLCLs from healthy and MDD donors have comparable levels of NR3C1 mRNA. Levels of NR3C2 are very low but also unchanged. (qPCR, n = 5 biological replicates, mean ± SEM).

(D) BLCLs from healthy and MDD donors have comparable levels of NR3C1 protein. (Western Blot quantification of NR3C1 relative to B-TUBULIN (BTUB), n = 5 biological replicates, mean ± SEM).

(E) BLCLs from healthy and MDD donors similarly upregulate FKBP5 and TSC22D3 after cortisol-treatment (100 nM). (qPCR, n = 5 biological replicates, mean ± SEM. 2-way ANOVA: "Cortisol effect" indicates a significant main effect of cortisol treatment: FKBP5 3 H: $F(1, 16) = 13.171$, $P < 0.001$, TSC22D3 1 hr: $F(1, 16) = 55.245$, $P < 0.001$, TSC22D3 3 H: $F(1, 16) = 71.518$, $P < 0.001$).

Figure S9

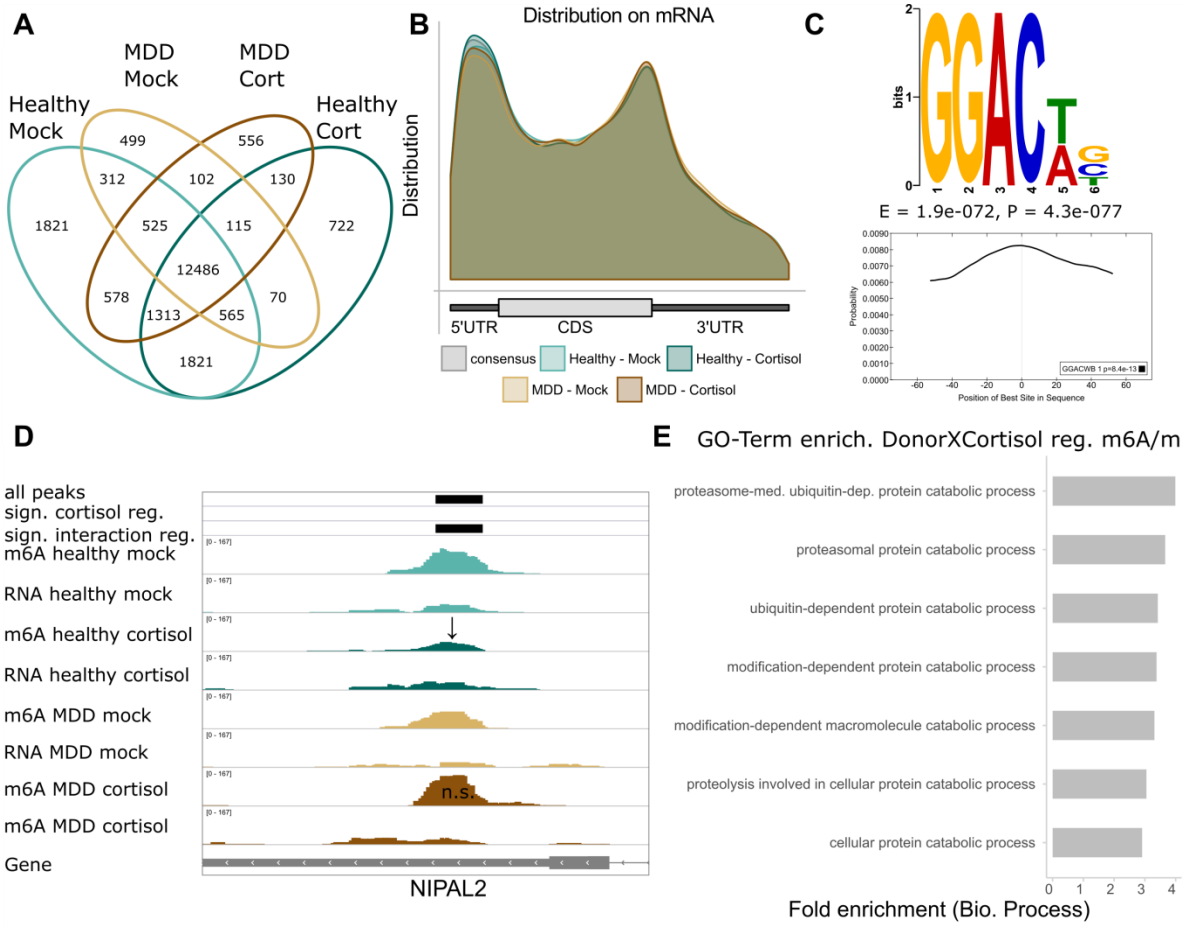

F

Gene	Peak position	Abundancy RNA (baseMean)	Main Cortisol log2FoldChange	Main Cortisol p.adjust	log2FoldChange in healthy	p.adjust in healthy	log2FoldChange in MDD	p.adjust in MDD
CLDN23	CDS	46.474	-1.135	0.001	-1.135	0.001	0.107	0.999
RNF139	5UTR	88.300	-1.068	0.022	-1.068	0.022	0.279	0.997
ZCCHC17	5UTR	211.817	-1.002	0.024	-1.002	0.024	0.047	0.999
TIFA	CDS	394.470	-0.795	0.006	-0.795	0.006	0.101	0.998
CEBPZ	CDS	195.307	-0.773	0.014	-0.773	0.014	0.076	0.999
RAP2B	3UTR	719.869	-0.762	0.000	-0.762	0.000	-0.118	0.998
QSER1	CDS	236.714	-0.753	0.066	-0.753	0.066	0.071	0.999
KLHL20	5UTR	139.908	-0.727	0.023	-0.727	0.023	0.015	0.999
STIL	CDS	430.128	-0.610	0.058	-0.610	0.058	0.066	0.999
KLLN	3UTR	214.924	0.709	0.000	0.709	0.000	0.077	0.998
SNX19	5UTR	890.917	0.743	0.037	0.743	0.037	-0.219	0.996
RC3H1	5UTR	498.403	0.777	0.093	0.777	0.093	0.042	0.999
C18orf25	5UTR	226.988	0.809	0.095	0.809	0.095	-0.169	0.998
SAP30	5UTR	269.402	0.849	0.049	0.849	0.049	-0.051	0.999
PPP2R3C	5UTR	50.407	0.863	0.008	0.863	0.008	0.215	0.997
ADAM10	5UTR	243.352	0.867	0.000	0.867	0.000	0.071	0.999
SLC15A4	5UTR	533.357	0.868	0.000	0.868	0.000	0.014	0.999
ZNF23	3UTR	46.897	0.873	0.087	0.873	0.087	-0.241	0.997
EIF4B	5UTR	3931.136	0.921	0.012	0.921	0.012	-0.106	0.998
FBXO22	5UTR	106.184	1.079	0.013	1.079	0.013	-0.117	0.999
MAPKAPK5-AS1	5UTR	51.716	1.139	0.027	1.139	0.027	0.160	0.998
RBM19	5UTR	1952.656	1.181	0.000	1.181	0.000	0.297	0.994
ENPP4	CDS	42.454	1.226	0.090	1.226	0.090	-0.049	0.999
PHF8	5UTR	1002.683	1.264	0.001	1.264	0.001	-0.081	0.999
AREG	5UTR	9.010	2.185	0.035	2.185	0.035	0.641	0.996

G

Gene	Peak position	Abundancy RNA (baseMean)	Main Cortisol log2FoldChange	Main Cortisol p.adjust	log2FoldChange in healthy	p.adjust in healthy	log2FoldChange in MDD	p.adjust in MDD
CLDN23	CDS	46.474	-1.135	0.001	-1.135	0.001	0.107	0.999
RNF139	5UTR	88.300	-1.068	0.022	-1.068	0.022	0.279	0.997
ZCCHC17	5UTR	211.817	-1.002	0.024	-1.002	0.024	0.047	0.999
TIFA	CDS	394.470	-0.795	0.006	-0.795	0.006	0.101	0.998
CEBPZ	CDS	195.307	-0.773	0.014	-0.773	0.014	0.076	0.999
RAP2B	3UTR	719.869	-0.762	0.000	-0.762	0.000	-0.118	0.998
QSER1	CDS	236.714	-0.753	0.066	-0.753	0.066	0.071	0.999
KLHL20	5UTR	139.908	-0.727	0.023	-0.727	0.023	0.015	0.999
STIL	CDS	430.128	-0.610	0.058	-0.610	0.058	0.066	0.999
KLLN	3UTR	214.924	0.709	0.000	0.709	0.000	0.077	0.998
SNX19	5UTR	890.917	0.743	0.037	0.743	0.037	-0.219	0.996
RC3H1	5UTR	498.403	0.777	0.093	0.777	0.093	0.042	0.999
C18orf25	5UTR	226.988	0.809	0.095	0.809	0.095	-0.169	0.998
SAP30	5UTR	269.402	0.849	0.049	0.849	0.049	-0.051	0.999
PPP2R3C	5UTR	50.407	0.863	0.008	0.863	0.008	0.215	0.997
ADAM10	5UTR	243.352	0.867	0.000	0.867	0.000	0.071	0.999
SLC15A4	5UTR	533.357	0.868	0.000	0.868	0.000	0.014	0.999
ZNF23	3UTR	46.897	0.873	0.087	0.873	0.087	-0.241	0.997
EIF4B	5UTR	3931.136	0.921	0.012	0.921	0.012	-0.106	0.998
FBXO22	5UTR	106.184	1.079	0.013	1.079	0.013	-0.117	0.999
MAPKAPK5-AS1	5UTR	51.716	1.139	0.027	1.139	0.027	0.160	0.998
RBM19	5UTR	1952.656	1.181	0.000	1.181	0.000	0.297	0.994
ENPP4	CDS	42.454	1.226	0.090	1.226	0.090	-0.049	0.999
PHF8	5UTR	1002.683	1.264	0.001	1.264	0.001	-0.081	0.999
AREG	5UTR	9.010	2.185	0.035	2.185	0.035	0.641	0.996

Figure S9. Additional analysis of m^{6}A/m-Seq of human BLCLs. Related to Figure 8.

(A) m^{6}A/m-peaks detected per group mostly overlap. Shown are number and overlap of detected peaks per group (in minimum 2/3 of the samples without additional abundancy filters applied to consensus peaks).

(B) m^6A/m-peaks detected per group as well as consensus peaks detected across all samples and used for differential methylation analysis have similar distribution as seen for mouse brain m^6A/m-peaks.
(C) Consistent with mouse brain m^6A/m, in human BLCLs GGACWB is the most abundant motif detected in m^6A/m-peaks and enriched at peak summits. Shown is the top detected sequence motif and its position across the detected m^6A/m-peaks.
(D) Example of an m^6A/m-peak regulated in a donor-specific fashion (downregulated in healthy donor cells but not in MDD donor cells). Shown are averaged sequence tracks m^6A/m-Seq and RNA-Seq per group and detected m^6A/m-peaks. Arrows indicate quantitatively regulated peaks ($Q < 0.1$, abs log2FC > 0.5).
(E) m^6A/m-peaks in BLCLs regulated by cortisol in a donor-specific fashion are enriched for genes with catabolic rather than metabolic functions. (Enriched Biological Process gene ontology (GO) terms. Overrepresentation test of m^6A/m-peaks in BLCLs compared to all genes detected in input samples with FDR-corrected $Q < 0.1$.)
(F) Top 25 regulated m^6A/m-peaks by cortisol.
(G) Top 25 regulated m^6A/m-peaks by cortisol in a donor-specific fashion.